Supporting Information

Ion-specific Ice Propagation Behavior on Polyelectrolyte Brush Surfaces

Zhenqi Liu, Zhiyuan He*, Jianyong Lv, Yuankai Jin, Shuwang Wu, Guangming Liu, Feng Zhou and Jianjun Wang*

Experimental Section

Materials. [2-(Methacryloyloxy)ethyl] trimethylammonium chloride (METAC, 80 wt % in H_2O, Sigma Aldrich), Copper bromide (CuBr, 99.999%, Sigma Aldrich), 2,2'-bipyridine (bpy, 99%, Aladdin), ethyl 2-bromoisobutyrate (2-EBiB, Sigma-Aldrich) were used as received. The bromo-substituted thiol initiator was synthesized by Suzhou Institute of Nano-Tech and Nano-Bionics. Milli-Q water was provided by a Millipore purification system. Sodium chloride (NaCl, 99.99%, Aladdin), sodium hexafluorophosphate ($NaPF_6$, 99%, J&K), bis(trifluoromethane) sulfonamide lithium (TFSI, 99.95%, Sigma Aldrich) and sodium perfluorooctanoate (PFO, 97%, J&K) were all purchased without further purification.

Preparation of PMETA Brushes. The PMETA brushes were prepared by a typical surface initiated atom transfer radical polymerization (SI-ATRP) method. Silicon wafers evaporation deposited with gold were immersed into the solution of the thiol initiator (1mg/mL) without stirring for 10 hours and rinsed with ethanol and water. The polymerization process was carried out as follows: METAC (90 mL, an 80 wt. % solution in water) and 2, 2'-dipyridyl (1.8g) were dissolved in the solvent of Milli-Q water (60 mL) and Methanol (30 mL). The mixture was freeze-pump-thaw degassed at

1

least three times. CuBr (0.525g) and initiator-coated samples were then added into the reaction vessel. The vessel was then degassed and left at room temperature in the argon protection environment. After polymerization, the samples were then preserved in a 0.5 M NaCl solution for further use after rinsed with ethanol and Milli-Q water. PMETA brushes with different thicknesses were achieved by adding extra amount of bulk polymerization initiator 2-EBiB and altering the polymerization time.

Ion-Exchange Process and XPS Results. The ion exchange process was carried out by immersing the PB into a solution of 0.1 M sodium/lithium salts for 8 hours (0.05M for PFO$^-$). After the counterion exchange, the samples were rinsed with Milli-Q water, ethanol and then N_2 dried. In order to remove excess surface free salts, the brush samples were subsequently rinsed with copious of Milli-Q water. According to X-ray photoelectron spectroscopy (XPS) results, it was proved that all the counterions were successfully exchanged in PMETA brushes as shown in Figure S1. The absence of signals of Na/Li indicated that free sodium/lithium cations inside the brush were completely removed.

Characterization The surface topologies were conducted on AFM (Bruker Multimode 8) equipped with liquid cell via 'peak force tapping mode'. AFM tips on a nitride cantilever (spring constant = 0.65N/m) were used to better probe the surface profile. Thickness measurement of the PB in both 'dry' state and 'wet' state were conducted *in-situ* by a spectroscopic ellipsometer (SE) (M-2000V, J. A. Woollam) with an incidence angle of 75° and the wavelength was varied from 370.1 to 999.1 nm in an aqueous medium. The well-established Cauchy model for transparent substrates was

used to fit the data, because there was no absorption of the incident light by the brush in the aqueous solution. For this model, the refractive index r was described as $r = A + \dfrac{B}{\lambda^2}$, where A, B were fitting parameters related to r. For measurements in the aqueous solutions, the parameter and thicknesses were set to be fitted due to the difference in refractive index between dry and wet PB. The static contact angle measurements were measured by a drop size analyzer (DSA-100, KRÜSS, Germany). The images were captured by an optical microscope precisely 30 seconds after the contact of a droplet with the PB surface.

Ice Propagation of Water Microdroplets and Macrodroplets. The freezing measurements of water microdroplets on PB surfaces were examined by using the method and apparatus previously reported (details in Figure S2),[1] a droplet of 0.4μL was placed at the edges of the PB surface to be tested and evaporated into a small chamber by elevating the temperature to 50.0 °C, then the chamber was cooled gradually to 5.0 °C and kept for 1h to let water condense. Due to the small volume of the chamber, the adequate water content and the long holding time, the condensed water droplets and the surrounding water vapor can be considered as isopiestic in vapor pressure. Then the sample cell was cooled to -20.0 °C at a very low speed of 1.0 °C/min. Hence all freezing events occurred in the water saturated environment, and the relative humidity (RH) can be approximately considered as 100%. In fact, it is so difficult to control the RH of the low-temperature environment as the temperature changes. So the fixed RH of 100% can make such complicated matters simplified.

Similarly, before the ice propagation measurements of the macrodroplets, the as-prepared samples with macrodroplets were kept for 1h at almost zero supercooling (heterogeneous ice nucleation temperature on the PMETA brush surfaces with different counterions was obtained via our previous experimental method)[2] to make sure that the environment reached the water saturated state without any evaporation or condensation. The ice propagation processes of both condensed microdroplets and macrodroplets were captured by a high speed camera (Phantom v7.3) at the speed of 300 frames per second.

Calculation of Frozen Droplet Ratio and Ice Propagation Rate. The freezing occurred as signified by the sudden increase in the opacity of water microdroplets. The frozen droplet ratios were calculated according to the analysis of many in situ time-resolved optical microscopic images of all the freezing events (see Fig. S4). The microscopic field of view was fixed in 800 μm × 600 μm. The corresponding ice propagation rates for each PB surface with different counterions were the sample means based on more than 20 independent experimental tests.
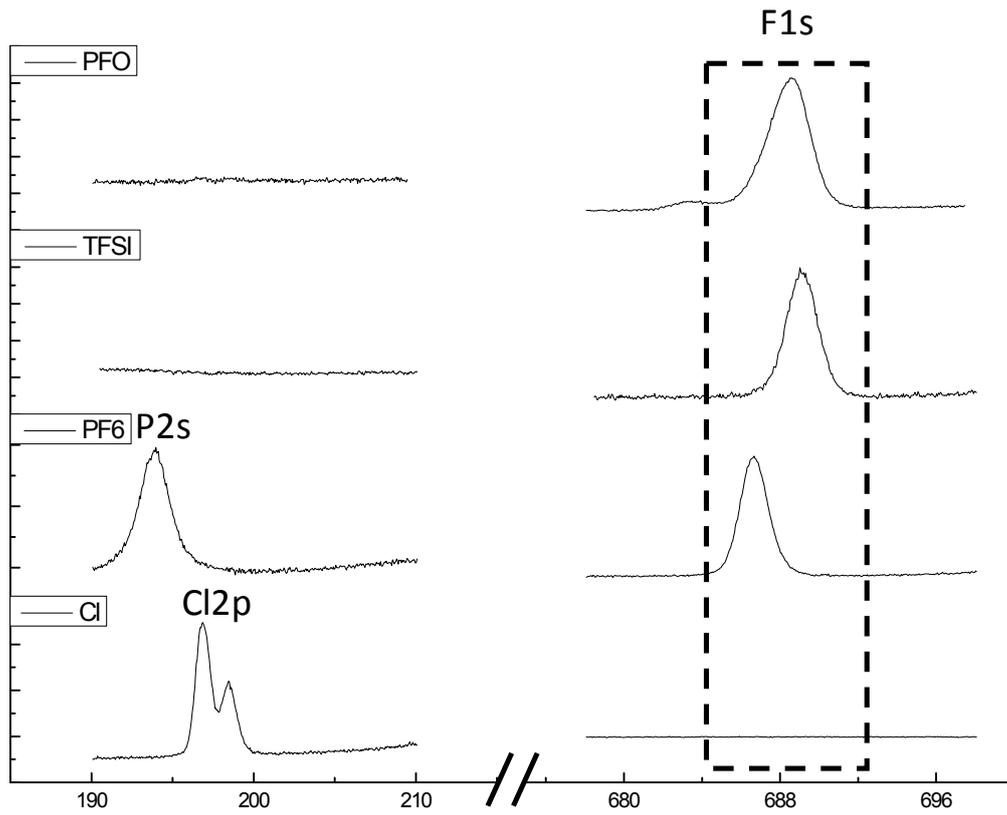
Figure S1 XPS data showed the PMETA brush has been successfully exchanged with different counterions of Cl^- , PF_6^- , $TFSI^-$ and PFO^- , respectively .
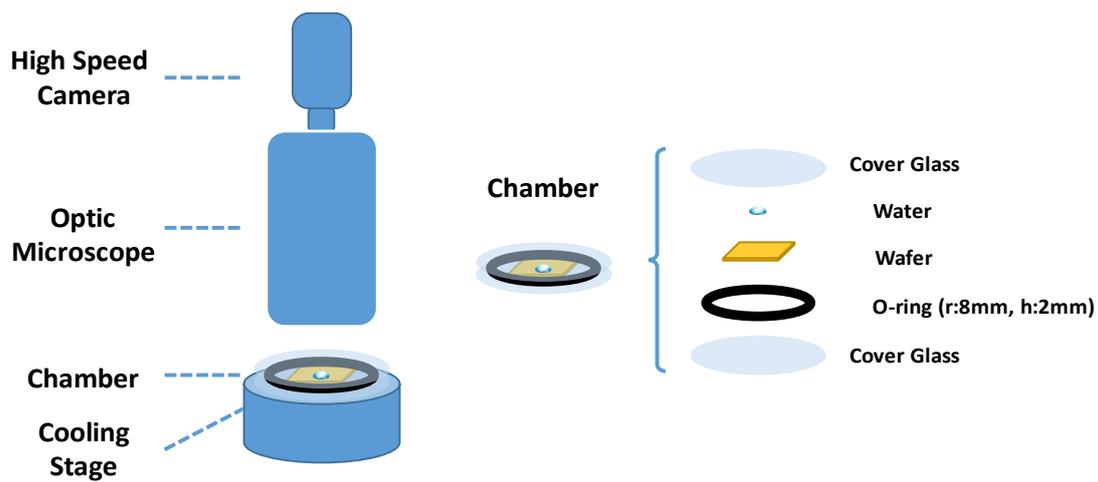
Figure S2. The home-made experimental apparatus used to detect ice propagation on PB surfaces. The sample cell was composed of a rubber O-ring sandwiched between two cover glasses.
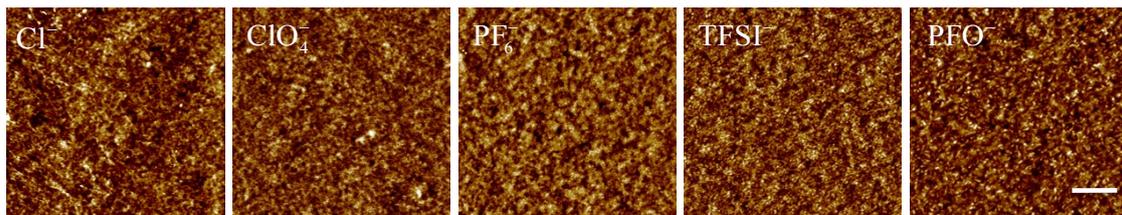
Figure S3. The surface morphology in water corresponding to PMETAC brushes with different counterions (Cl^-, ClO_4^-, PF_6^-, $TFSI^-$ and PFO^-). The grafting densities are all 0.50 chain/nm^2. The scale bar of AFM height images is 1 μm.
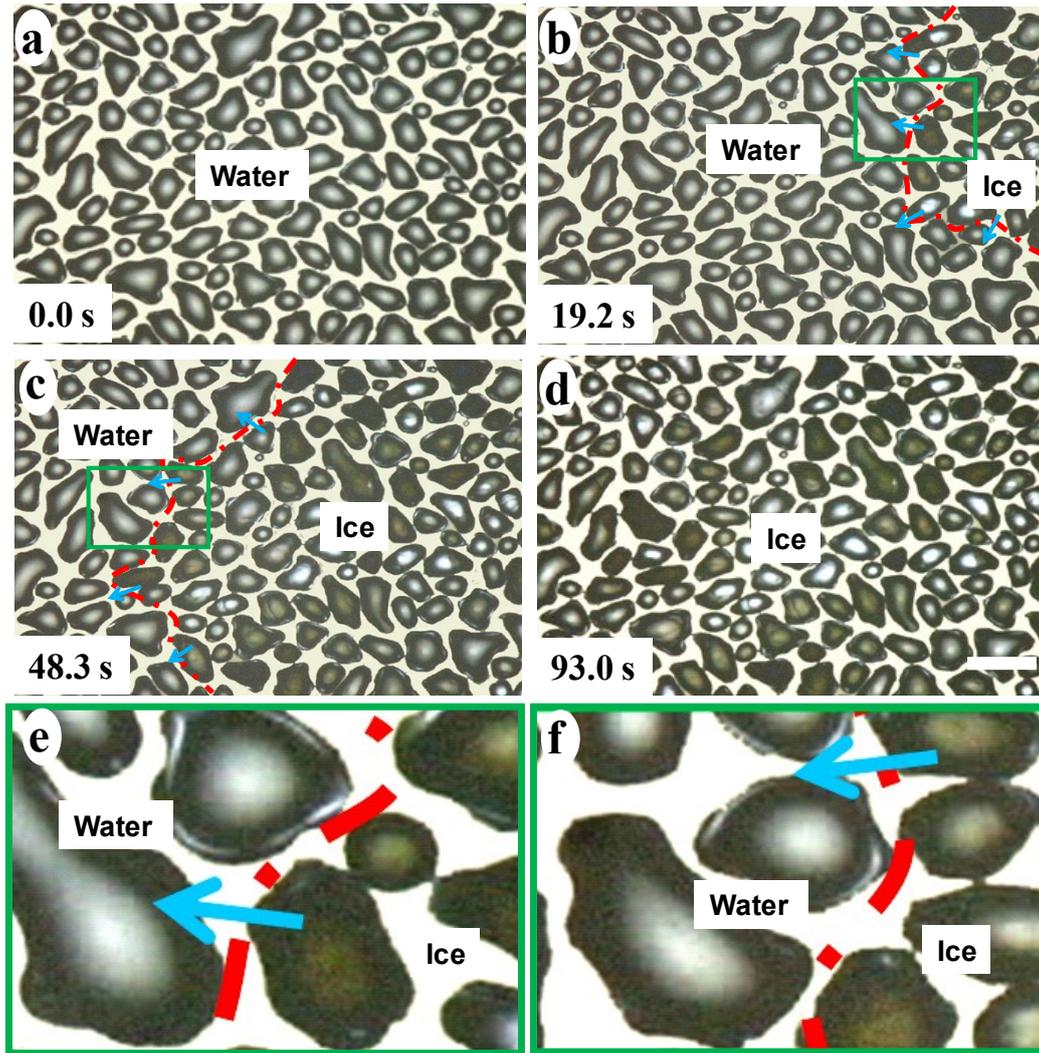
Figure S4. The time-resolved optical microscopic images of ice propagation on the PMETA-PFO surface at a) 0.0s, b) 19.2s, c) 48.3s and d) 93.0s (The scale bar is 100 μm.). The red dash lines denote the ice propagation frontier, and the blue arrows denote the ice propagation direction. The frozen droplets locate on the right side of the red line, and the unfrozen droplets locate on the left side of the red line, respectively. The magnified fig. e and f which show the details of ice propagation correspond to the inset green square in fig. b and c, respectively.

193 independent microdroplets are counted to calculate the frozen droplet ratio by a high speed camera as shown in Figure S4. In the initial state at 0.0s, all the microdroplets are unfrozen and the frozen droplet ratio is 0.0. As shown in Fig. S4b, 30 water droplets freeze

after 19.2s, and the frozen droplet ratio is 0.22. 92 water droplets freeze after 48.3s as shown

in Fig. S4c, and the frozen droplet ratio becomes 0.66. All the 193 microdroplets are frozen

within 93.0s as shown in Fig. S4d, and the frozen droplet ratio is 1.0.
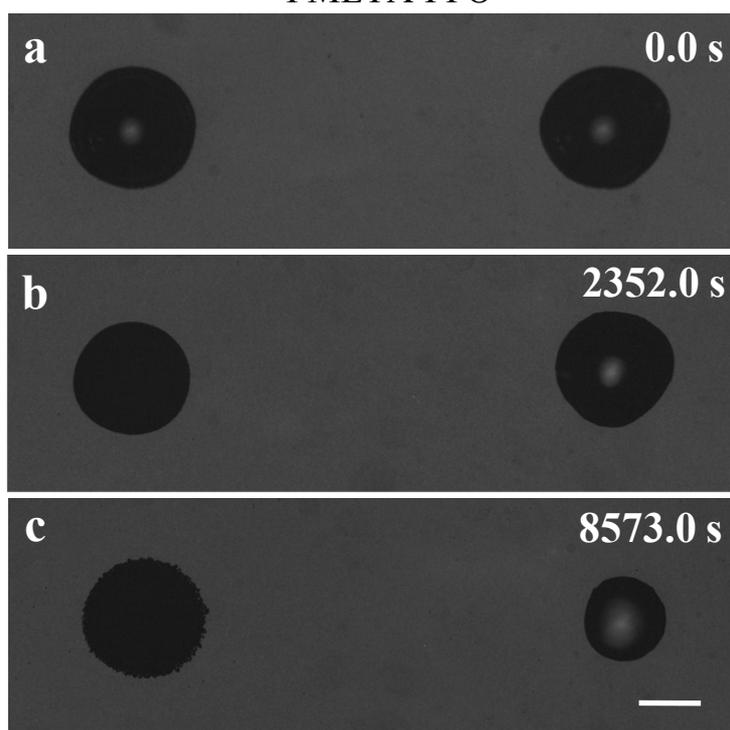
PMETA-PFO

Figure S5. Optical images of two water macroscopic droplets frozen at -20.0 °C on brush surfaces of PMETA-PFO for a) 0.0 s, b) 2352.0 s, c) 8573.0 s. When the difference of freezing time between frozen (left) and unfrozen (right) droplets is great, the unfrozen water droplet decreased in size due to evaporation. The scale bar is 1.0 mm.

Reference

1. K. Li, S. Xu, W. Shi, M. He, H. Li, S. Li, X. Zhou, J. Wang and Y. Song, *Langmuir*, 2012, **28**, 10749.

2. Z. He, W. J. Xie, Z. Liu, G. Liu, Z. Wang, Y. Q. Gao and J. Wang, *Science Advances*, 2016, **2**.